journal

J. Am. Ceram. Soc., 76 [11] 2817–25 (1993)

Thermomechanical Fatigue Behavior of a Silicon Carbide Fiber-Reinforced Calcium Aluminosilicate Composite

Lawrence M. Butkus*,† and John W. Holmes*

Ceramic Composites Research Laboratory, The University of Michigan, Ann Arbor, Michigan 48109

Theodore Nicholas

Materials Behavior Branch, Materials Directorate, WL/MLLN, Wright-Patterson AFB, Ohio 45433–6533

Isothermal fatigue and in-phase thermomechanical fatigue (TMF) tests were performed on a unidirectional, continuous-fiber, Nicalon®-reinforced calcium aluminosilicate glass-ceramic composite ($[0]_{16}$, SiC/CAS-II). Monotonic tensile tests were performed at 1100°C (2012°F) and 100 MPa/s (14.5 ksi/s) to determine the material's ultimate strength (σ_{ult}) and proportional limit (σ_{pl}). Isothermal fatigue tests at 1100°C employed two loading profiles, a triangular waveform with ramp times of 60 s and a similar profile with a superimposed 60-s hold time at σ_{max}. All fatigue tests used a σ_{max} of 100 MPa (40% of σ_{pl}), $R = 0.1$. TMF loading profiles were identical to the isothermal loading profiles, but the temperature was cycled between 500° and 1100°C (932° and 2012°F). All fatigued specimens reached run-out (1000 cycles) and were tested in tension at 1100°C immediately following the fatigue tests. Residual modulus, residual strength, cyclic stress–strain modulus, and strain accumulation were all examined as possible damage indicators. Strain accumulation allowed for the greatest distinction to be made among the types of tests performed. Fiber and matrix stress analyses and creep data for this material suggest that matrix creep is the primary source of damage for the fatigue loading histories investigated.

I. Introduction

MAN-MADE composite materials have been in use for thousands of years. Presently, new forms of high-temperature composites, ceramic matrix composites (CMCs), are receiving a great deal of research emphasis. The attraction to ceramic composites is most evident in the aerospace industry, where their use promises structural weight savings as well as greater engine efficiencies resulting from increased maximum operating temperatures.

Ceramic matrix composites combine the high specific strengths and moduli characteristic of reinforcing carbon or silicon carbide fibers, with the high-temperature capabilities associated with the parent glass, glass-ceramic, or ceramic matrix. This synergy has made CMCs one of the enabling technologies for advanced turbine engines, hypersonic vehicles, and space applications.

Prior to the use of CMCs in structures or powerplants, their mechanical and thermal properties must be extensively investigated. Of particular interest to aircraft engine designers are the fatigue and creep properties of these new materials. Although many investigations of the mechanical properties of ceramic composites have been performed (Refs. 1–8 offer a brief sample), the fatigue properties of CMCs have been explored in a limited, though growing, number of studies.[9–12] A few works have also examined the thermal fatigue[13] and creep behavior[14,15] of ceramic composites. Interest has been focused on the cyclic accumulation of damage within ceramic composites en route to the future life-prediction models required by design engineers. Crucial questions have arisen regarding the behavior of CMCs under conditions representative of the combined mechanical and thermal loadings present in turbine engines, often termed thermomechanical fatigue (TMF) conditions.

This paper will present the results of a recent research program which examined the behavior of a 16-ply unidirectional Nicalon® fiber-reinforced calcium aluminosilicate glass-ceramic (SiC/CAS-II, $[0]_{16}$) subjected to several thermomechanical loading histories. A total of 11 specimens were tested for this project under the conditions shown in Table I.

This program was a cooperative effort between the University of Michigan's Ceramic Composites Research Laboratory and the Materials Behavior Branch of the Materials Directorate (Wright Laboratory, Wright-Patterson AFB, OH.) The purpose of this project was threefold. The primary objective was to establish and demonstrate the capability of performing thermomechanical fatigue testing on CMCs. Based on an extensive literature review, it appears that the TMF experiments conducted for this project are the first of their kind for ceramic matrix composites. The second objective was to investigate the isothermal and thermomechanical fatigue behavior of SiC/CAS-II material. The final objective was to acquire and analyze data which might explain damage initiation and accumulation occurring during the specified profiles.

II. Experimental Procedure

(1) Material

The material used in this project was a ceramic-grade Nicalon® (Code NL-202, Nippon Carbon Co. Ltd, Yokohama, Japan) fiber-reinforced calcium aluminosilicate glass-ceramic composite designated SiC/CAS-II (Corning Glass Works, Corning, NY) (Fig. 1). The composite was supplied in 16-ply, unidirectionally reinforced ($[0]_{16}$) panels, measuring 152.4 cm × 152.4 cm (6 in. × 6 in.). This material was produced by hot-pressing, using prepregged unidirectional plies approximately 0.56 mm (0.022 in.) thick and fabricated using 500-count fiber tows. The hot-pressing temperature was approximately 1350°C (2462°F). The resulting composite had an approximate fiber volume fraction of 40%.

W. K. Tredway—contributing editor

Manuscript No. 195601. Received June 12, 1992; approved December 28, 1992.
Presented in part at the 16th Annual Conference on Composites and Advanced Ceramics, Cocoa Beach, FL, January 14, 1992 (Paper No. CB92-134).
Based upon the thesis submitted by L. M. Butkus for the M.S. degree in Mechanical Engineering, University of Michigan, Ann Arbor, MI, December 1991.
Supported by the Ceramic and Nonmetallic Structural Materials Branch, Air Force Office of Scientific Research, Grant No. 91-0106.
*Member, American Ceramic Society.
†Presently, Instructor, Department of Engineering Mechanics, HQ USAFA/D-FEM, U.S. Air Force Academy, CO 80840.

Table I. Test Matrix and Summary of Results

Specimen No. (plate-specimen)	Test type	Temp (°C) [°F]	Ramp/profile	Max stress (MPa) [ksi]	Initial modulus (MPa) [ksi]	Residual strength (MPa) [ksi]	Residual modulus (GPa) [Msi]	Location of failure
9032005L-07	Tens.	23 [73]	100 MPa/s	552 [80.1]	131 [129]			Within specimen gage length
9032005L-01	Tens.	1100 [2012]	100 MPa/s	381 [55.3]	134 [19.4]			Within extensometer gage length
9032006L-10	Tens.	1100 [2012]	100 Mpa/s	341 [49.5]	129 [18.7]			Outside of gage lengths (in radius)
9032006L-01	Tens.	1100 [2012]	100 MPa/s	361 [52.4]	131 [129]			Within specimen gage length
9032005L-10	ITF	1100 [2012]	60-s ramp, no hold, $R = 0.1$	100 [14.5]		343 [49.7]	105 [15.2]	Within extensometer gage length
9032005L-09	ITF	1100 [2012]	60-s ramp, w/hold, $R = 0.1$	100 [14.5]		339 [49.2]	112 [16.2]	Within specimen gage length
9032005L-09	ITF	1100 [2012]	60-s ramp, w/hold, $R = 0.1$	100 [14.5]		276 [40.0]	112 [16.2]	Within specimen gage length
9032005L-08	TMF	500–1100 [932–2012]	60-s ramp, no hold, $R = 0.1$	100 [14.5]		364 [52.8]	110 [16.0]	Outside of gage lengths (in radius)
9032007L-04	TMF	500–1100 [932–2012]	60-s ramp, no hold, $R = 0.1$	100 [14.5]		364 [52.8]	97 [14.1]	Within specimen gage length
9032005L-06	TMF	500–1100 [932–2012]	60-s ramp, w/hold, $R = 0.1$	100 [14.5]		341 [49.5]	115 [16.7]	Within specimen gage length
9032006L-07	TMF	500–1100 [932–2012]	60-s ramp, w/hold, $R = 0.1$	100 [14.5]		297 [42.2]	110 [16.0]	Outside of gage lengths (in radius)

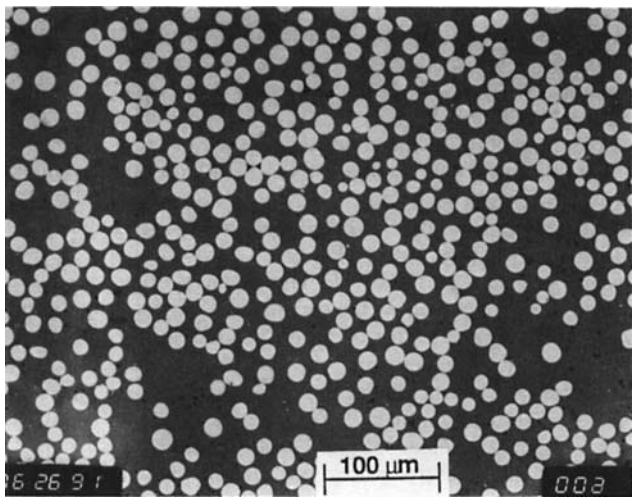

Fig. 1. Microstructure of SiC/CAS-II, transverse view.

A reaction between the matrix and fiber during fabrication forms a carbon-rich fiber–matrix interface *in situ* as carbon leaches out of the Nicalon® fibers.[16]

Reported fiber, matrix, and composite properties are shown in Table II.

Surface replicas of unloaded specimens revealed no matrix cracking in the as-received material.

CAS-II has a strain point temperature[‡] of 1260°C (2300°F) and a liquidus temperature[§] of 1520°–1540°C (2768°–2804°F).[17] It is regarded as well-suited for use in composites because of its low processing temperature (which minimizes fiber damage), ability to be tailored in composition to obtain specific properties,[18] and superior high-temperature performance.[19] Although possessing the glasslike ability to flow around fibers while molten (resulting in low porosity), it is semicrystalline in its final state, having partially crystallized during heat treatment ("ceramming").[20]

(2) Specimen Design

Edge-loaded test specimens (Fig. 2) were designed based upon a geometry optimized by Ma *et al.*[21,22] for use with CMCs with low interfacial shear strengths. The specimens had a 33-mm (1.3-in.) gage section and were machined from composite panels using precision diamond grinding machines holding dimensional tolerances of ±0.1 mm (±0.004 in.) and angular tolerances of ±2 min. Faces were left in the as-pressed condition of the parent panels.

(3) Test Procedures

Monotonic tensile, isothermal fatigue, and in-phase TMF tests were conducted in air under load control. Isothermal tensile tests were conducted at 1100°C (2012°F) and at room temperature (23°C (73°F)) to determine the material's ultimate strength (σ_{ult}) and proportional limit (σ_{pl}). The loading rate used was equivalent to a stress rate of 100 MPa/s (14.5 ksi/s). This relatively high loading rate was chosen to minimize creep effects[23] and to prevent rate-dependent interfacial shear strength variations[24] from influencing the elevated temperature tensile behavior of the material.

Isothermal fatigue tests were conducted at 1100°C utilizing two loading profiles: a triangular profile consisting of 60-s ramps with a maximum stress of 100 MPa, and an identical profile with a superimposed 60-s hold time at σ_{max} (Fig. 3). Isothermal fatigue tests were conducted using an R value of 0.1 (defined as the ratio $\sigma_{min}/\sigma_{max}$). The maximum stress of 100 MPa was chosen as 40% of the proportional limit at 1100°C. Run-out was defined as 1000 cycles, corresponding to 33.3 h of testing using the triangular profiles and 50 h of testing using the

[‡]The strain point temperature is the temperature at which CAS-II has a viscosity of 10^{12} poise (10^{11} Pa·s). Above this temperature (below this viscosity), the matrix loses its ability to retain stresses.

[§]The liquidus temperature is that at which CAS-II begins to solidify from the melt upon cooling.

Table II. Selected Fiber, Matrix, and Composite Properties

Property*,†	Fiber‡ Nicalon® NL-202	Matrix§ CAS-II	Composite§,¶ SiC/CAS-II, $[0]_{16}$
Density	2.55 g/cm³ (0.0092 lb/in³)	2.80 g/cm³ (0.0101 lb/in³)	2.70 g/cm³ (0.0098 lb/in³)
CTE (25°–1000°C) (77°–1832°F)	4.0 × 10^{-6}/°C (7.2 × 10^{-6}/°F)	5.01 × 10^{-6}/°C (9.02 × 10^{-6}/°F)	4.6 × 10^{-6}/°C (8.3 × 10^{-6}/°F)
Elastic modulus	193 GPa (28 Msi)	98 GPa (14 Msi)	131–138 GPa (19–20 Msi)
Poisson's ratio	0.2	0.26	0.25
Tensile strength	2520–3290 MPa** (365–477 ksi)		448–597 MPa (64–87 ksi)
4-point flex strength		133 MPa (193 ksi)	

*At 25°C unless noted. †Data supplied by Corning, Inc., Corning, NY, unless noted. ‡Manufactured by Nippon Carbon Co. Ltd., Yokohama, Japan. §Manufactured by Corning. ¶Data for SiC/CAS-II with 35% fiber volume. **T. Mah, M. G. Mendriatta, A. P. Katz, and K. S. Mazdiyasni, "Recent Developments in Fiber-Reinforced High Temperature Ceramic Composites," *Am. Ceram. Soc. Bull.*, **66**[2]304 (1987).

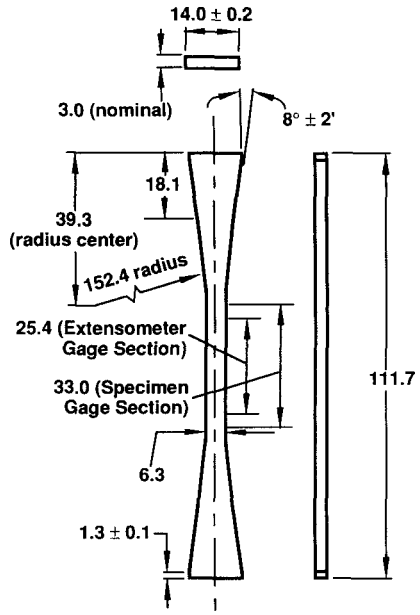

Fig. 2. Edge-loaded test specimen geometry. All dimensions in millimeters.

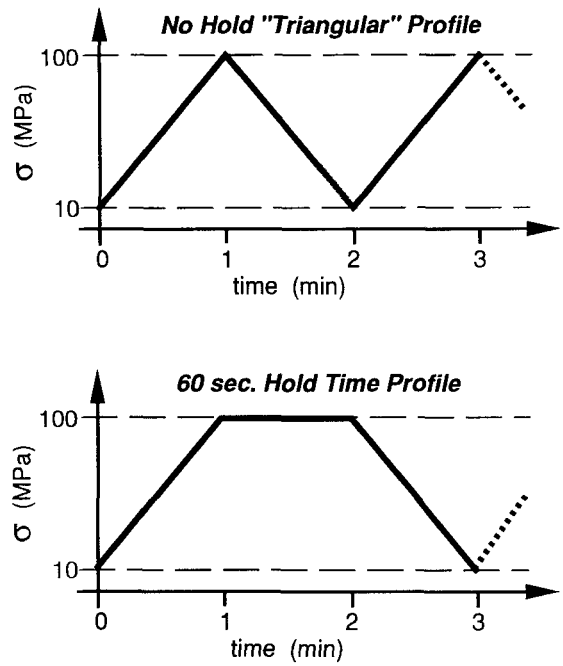

Fig. 3. Loading profiles for fatigue tests.

hold-time profile. Following 1000 fatigue cycles, the specimens were immediately subjected to tensile testing at 1100°C and 100 MPa/s.

Identical loading profiles were used for the thermomechanical fatigue tests. TMF test temperatures were cycled between a T_{min} of 500°C (932°F) and a T_{max} of 1100°C and were synchronized with the loading profiles to produce "in-phase" TMF tests. TMF run-out conditions and the postfatigue tensile testing procedure were identical to those used in the isothermal fatigue tests. TMF stress levels and temperatures were chosen based upon (1) estimated maximum use temperatures provided by the manufacturer, (2) creep performance of the SiC CAS-II composite, and (3) an estimated temperature profile of 500° to 1100°C in metallic turbine blades.[25] Temperature excursions occur much faster and TMF conditions are more complex in actual turbine engines, but test temperature ramp speeds were chosen to permit rapid cycle times while maintaining adequate temperature control.

(4) Test System Overview

The task of accurately determining thermomechanical properties of ceramic matrix composites is challenging. Mechanical testing for this project was carried out in the Materials Behavior Branch of the Materials Directorate (Wright-Patterson AFB, OH). The test station used was a horizontal servohydraulic system (Figs. 4 and 5) consisting of a test frame built in-house at the Materials Directorate, equipped with a 25-kN load cell and a 100-kN actuator (Model 244.21, Materials Testing Systems, Minneapolis, MN) fitted with an antirotation device. The station is controlled by a closed-loop controller (Model 458.20, Materials Testing Systems) and the Materials Analysis and Test Environment (MATE) (Version 3.6, University of Dayton Research Institute, Dayton, OH) data-acquisition and test control software. Further details of the experimental equipment can be found in Refs. 26–29.

(5) Grip System

The test station utilized a rigid grip system (Fig. 5). The grips were rigidly fixed to the actuator and load cell. For this project, the grip bodies were not actively cooled, based upon experimental experience which showed a greater percentage of gage section failures using uncooled or heated grips.[22] Thermocouple readings indicated grip temperatures on the face closest to the heated zone ranged from 165°C (330°F) for a specimen

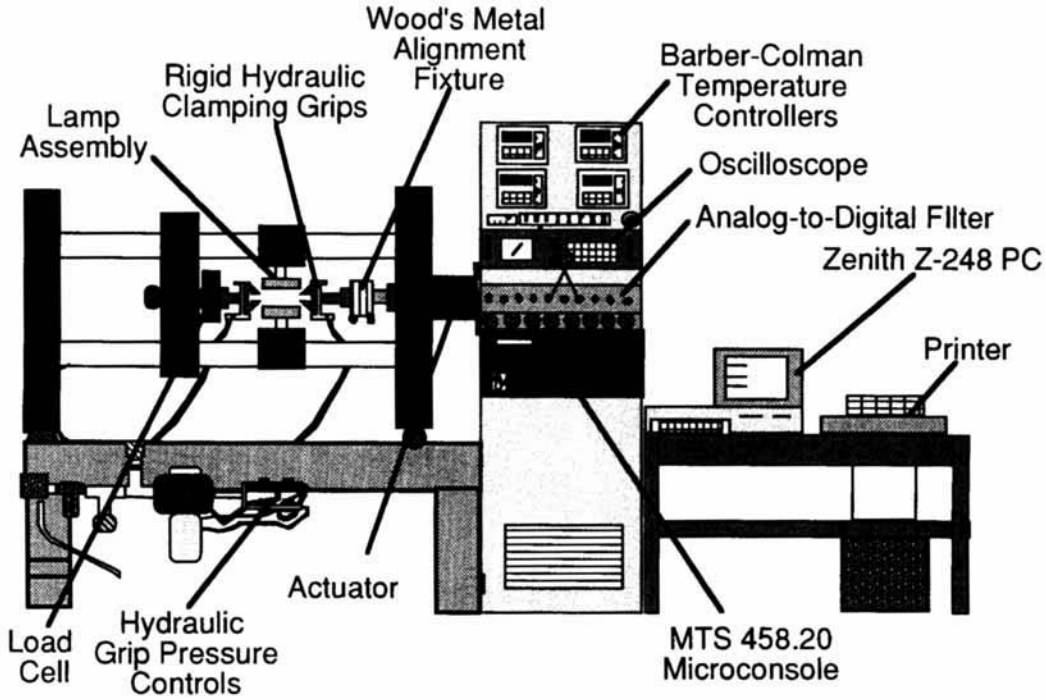

Fig. 4. Horizontal servohydraulic test machine.

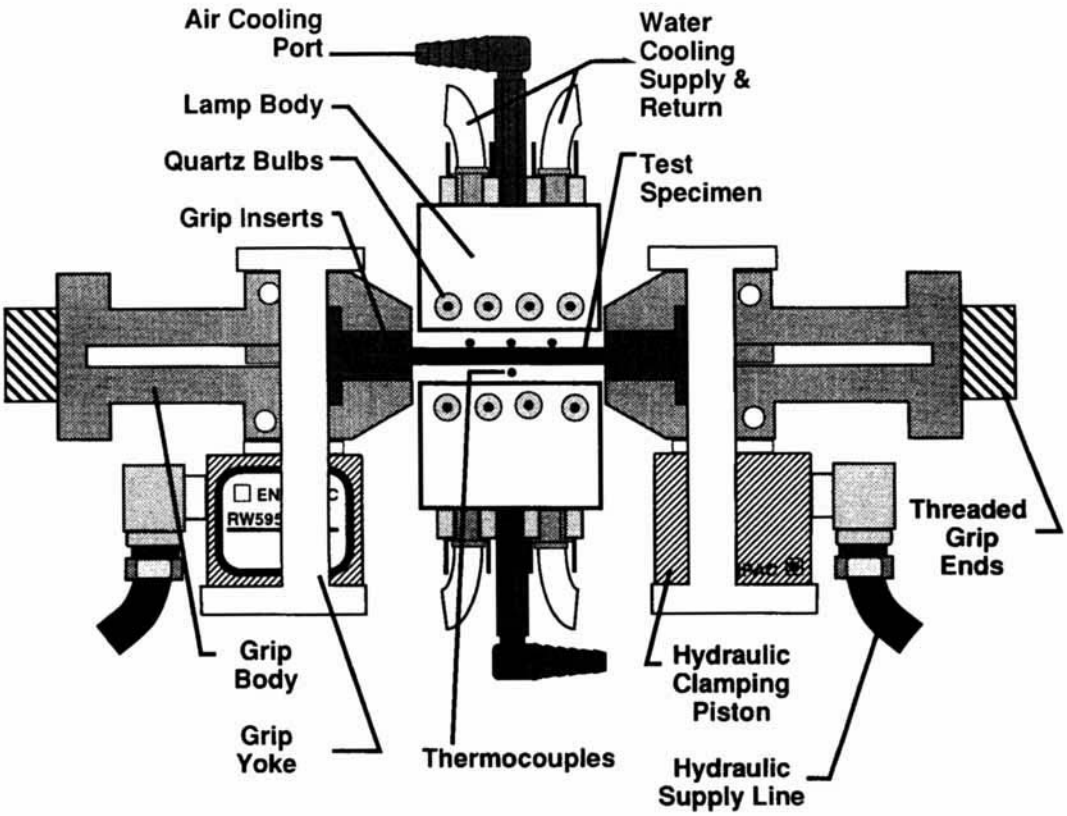

Fig. 5. Detail of grip system.

temperature of 500°C, to 260°C (500°F) for a specimen temperature of 1100°C.

Evaluations of bending due to load train misalignment following ASTM E1012-89 showed that bending strains were much less than 1% of total axial strains at test loads.

(6) Strain Measurement

Strain was measured using a 25.4-mm (1.0-in.) gage length elevated-temperature extensometer (Model 632.50B-01, Materials Testing Systems) that was air-cooled and equipped with 5-mm (0.197-in.) alumina (Al_2O_3) rods with conical points.

The extensometer was mounted on one side of the specimen, using a mounting spring force of 175 g (0.386 lb·ft). Calculations show that this configuration results in a bending strain of less than 5.5×10^{-4}% on uncracked specimens.

(7) Heating Technique and Temperature Measurement

Specimen heating was accomplished using two banks of four high-intensity (1000-W) tungsten-filament quartz bulbs placed above and below the specimen and oriented perpendicular to the loading axis (Fig. 5). Reflectors contained within the lamp bodies focused radiant energy upon the test specimen.

The eight bulbs were paired into four groups of two, or "zones" to allow temperature control at four points along a specimen (Fig. 5). A dedicated PID-based (proportional/integral/derivative) temperature controller (Model 560, Barber-Colman, Loves Parks, IL) and the MATE software provided temperature control for each of the four zones. Temperature deviations from the setpoint and gradients within the extensometer gage length of less than ±4°C (±7°F) were confirmed by multiple thermocouples and temperature-sensitive paint.

Each control zone was monitored by a beaded S-type (platinum/platinum–15%rhodium) thermocouple. Thermocouples were affixed to the surface of the specimen, using a wire holder made from K-type thermocouple wire and coated with a water-based alumina ceramic adhesive (Cotronics 903®, Cotronics, Brooklyn, NY). Portions of the thermocouple leads located within the lamp zone were shielded from test temperatures by alumina tubes.

(8) Data Acquisition and Test Control

Tests were controlled and data acquired using the MATE system software[26–29] linked to the test frame through an A/D (analog-to-digital) board. Long-term stability and repeatability of the data acquisition system have been previously demonstrated by Zawada *et al.*[30]

III. Results and Discussion

(1) Tensile Behavior

A single tensile test conducted at room temperature (23°C (73°F)) showed an initial material modulus, E_i, of 131 GPa (19 Msi) (Fig. 6). This value agrees closely with modulus data supplied by Corning, Inc. (131 to 138 GPa (19 to 20 Msi)), with that determined by Wang and Parvizi-Majidi (131.8 GPa (19.11 Msi)),[31] and with the value calculated using the "rule of mixtures" method (136 GPa (19.7 Msi)). The observed ultimate strength, σ_{ult}, of 552 MPa (80 ksi) is also within the range reported by Corning (448 to 597 MPa (65.5 to 86.6 ksi)) as is the observed strain at failure, e_{ult}, of 1.05% (Corning's data: 0.74% to 1.20%). The proportional limit, σ_{pl}, (the stress at which the stress–strain curve first deviates from linearity) occurred at 285 MPa (41 ksi), a higher level than that reported by Corning (173 to 217 MPa (25.1 to 31.5 ksi)). However, precision strain measurements conducted by Southern Research Institute[32] have shown that a deviation from linearity occurs as low as 68.9 MPa (10 ksi) in some SiC/CAS composites. Matrix microcracking has been observed in this composite system at stresses ranging from 120 to 150 MPa (17.4 to 21.8 ksi).[33,34]

Three stress–strain curves for specimens tested in tension under load-rate control at 1100°C are also shown in Fig. 6. These specimens exhibited an average initial modulus, E_i, of 130 GPa (18.9 Msi), similar to that of the room-temperature test. The average ultimate strength, σ_{ult}, of 361 MPa (52.4 ksi), average strain at failure, e_{ult}, of 0.58%, and proportional limit, σ_{pl}, of 249 MPa (36 ksi) are all lower than room-temperature values.

Optical inspection of the fracture surfaces revealed that the specimens tested at 1100°C exhibited approximately 10 mm (0.394 in.) of fiber pullout, whereas those tested at room temperature exhibited approximately 1.5 mm (0.059 in.) of pullout. Although studies have indicated that exposure to temperatures above 800°C (1472°F) strengthens some fiber–matrix interfaces, thereby reducing fiber pullout,[35,36] it appears that the mismatch between the coefficients of thermal expansion (CTE) of the fiber and matrix negates this behavior. The difference between the thermal expansion coefficients causes the matrix to contract and apply a compressive radial stress to the fiber during cool-down following processing. Calculations performed using a plane-strain, two-dimensional concentric cylinder model[37] indicate that this compressive stress rises to approximately 53 MPa (7.7 ksi) at room temperature. As the composite is reheated to 1100°C, this stress falls to approximately 6 MPa (0.87 ksi). The stronger fiber–matrix mechanical bond at lower temperatures may permit cracks to propagate from the matrix directly through the interface and into the fiber, resulting in less fiber pullout. A similar correlation between fiber pullout and CTE mismatch has been seen by Deshmukh *et al.*[38] In addition, the high loading rate (100 MPa/s) used in this project reduced the length of time for which the fibers were exposed to an oxidizing environment due to matrix cracks. Such an exposure time limit may account for the apparent dominance of the CTE mismatch effect over environmentally governed compositional changes influencing interfacial strength.

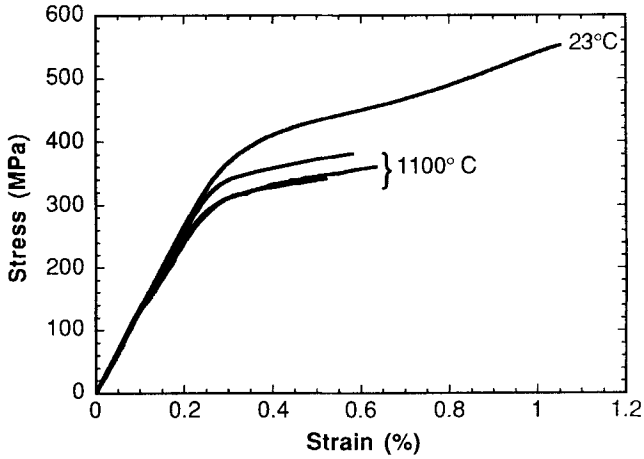

Fig. 6. Tensile behavior of $[0]_{16}$ SiC/CAS-II at 23° and 1100°C. Tests performed in air with a loading rate of 100 MPa/s.

(2) Fatigue Behavior

Figure 7 illustrates the typical mean mechanical strain history of unidirectional SiC/CAS-II for the isothermal and thermomechanical fatigue conditions used in this program. The mean strain is based upon the strains occurring at the maximum and minimum stresses recorded on any complete cycle. Strain accumulation illustrates the distinctions between the material behavior under various test conditions.These strains are referenced to the strain in the initial state of the material at the beginning of each test (10 MPa), and have had the thermal strains removed. Figure 7 will be referred to throughout the discussion of material behavior under isothermal and thermomechanical fatigue conditions.

(3) Isothermal Fatigue Behavior

A slight difference was observed between the maximum mean strains attained after 1000 cycles for the two types of isothermal fatigue tests performed. The specimen subjected to the 60-s hold-time cycle exhibited a maximum mean strain of nearly 0.25%, whereas the specimen subjected to the cyclic loading without a hold time attained a maximum strain of only 0.2% (Fig. 7). The difference in strain accumulation appears to be caused by the additional time under load. A comparison of the responses of these two specimens reveals that the amount of strain accumualted after identical times at the maximum stress is roughly the same. The specimen subjected to the cycle with the hold time also exhibited a slightly more rapid increase in

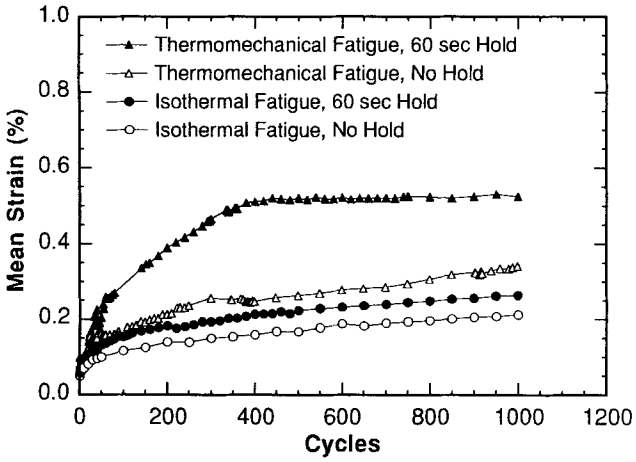

Fig. 7. Mean mechanical cyclic strain response of $[0]_{16}$ SiC/CAS-II for all fatigue profiles. σ_{max} = 100 MPa, R = 0.1.

accumulated strain than did the material subjected to the triangular waveform. This behavior suggests a more rapid accumulation of creep-induced strain caused by the hold time in the early phase of these isothermal tests. Since creep strain accumulation depends on stress level and time, the hold time at maximum stress is expected to cause a greater strain accumulation than will an equivalent number of triangular cycles.

No significant modulus changes were observed in any of the isothermal fatigue tests. Tension–tension fatigue testing performed by Prewo *et al.*[8] on SiC/LAS, Holmes *et al.*[9] on SiC/Si_3N_4, Zawada *et al.*[30] on SiC/aluminosilicate, and Butkus *et al.*[39] on SiC/CAS have all shown that material modulus is affected very little, if at all, by maximum stress values lower than the proportional limit stress. Presumably, this is because of the low levels of fiber damage and matrix cracking occurring at these stress levels. Recalling that the maximum fatigue stress level is 100 MPa and that the proportional limit stress at 1100°C is 250 MPa, the observed lack of a modulus reduction is to be expected. Based on the relatively constant value of the modulus throughout the isothermal tests, we may attribute the strain accumulation seen in Fig. 7 entirely to the accumulation of creep strains.

(4) Thermomechanical Fatigue Behavior

Trends analogous to those exhibited by the isothermal fatigue response of this material are evident in the mean strain responses to the two TMF profiles (Fig. 7). A higher level of accumulated strain and a more rapid cyclic rate of strain accumulation are evident in the thermomechanical profile, which includes the hold time. However, the strain accumulation is significantly greater in the TMF tests than in the isothermal tests under identical loading conditions, despite the fact that the composite spends less time at the peak temperature of 1100°C in the TMF tests. The triangular TMF loading condition resulted in a maximum mean mechanical strain of 0.34%, 60% greater than the corresponding strain for the triangular isothermal fatigue profile. A similar comparison between the hold profiles reveals that the thermomechanical fatigue test resulted in nearly twice as much strain accumulation as the isothermal fatigue test. In addition, the effect of the superimposed hold time under TMF conditions is much more dramatic, causing the maximum mean mechanical strain level for the material subjected to the hold time to be nearly 50% greater than for the material subjected to the triangular TMF profile.

Observed, also, is a behavior unseen in the isothermal fatigue tests: a saturation of strain accumulation for the composite subjected to the TMF profile including the hold time. This may be caused by the saturation of the matrix creep strain, resulting in the load being carried primarily by the fibers. These effects may become more pronounced in future tests performed with higher maximum stresses, stress ratios, and longer hold times.

Like the cyclic stress–strain moduli observed in the isothermal fatigue tests, the average TMF modulus values remained relatively constant during each test. This may indicate that damage is not occurring as matrix cracking but, rather, as permanent deformation due to creep. The increased rate and amount of strain accumulation in the TMF tests with the hold time, and the lack of modulus change during TMF tests, suggest that strain accumulation may be used as a damage indicator for these thermomechanical tests. As in the case of the isothermal fatigue tests, matrix creep appears to be the primary damage mechanism.

(5) Postfatigue Tensile Behavior

Immediately following the completion of 1000 cycles of isothermal or thermomechanical fatigue testing, specimens were tested in tension at 1100°C and 100 MPa/s to determine their residual strength and initial stress–strain moduli. These values, along with fracture locations, are listed in Table I. Three of the eleven tested specimens failed outside of the specimen gage sections in the radius.

Figures 8 and 9 show the average initial moduli and ultimate strengths for all tensile tests performed during this investigation. Average residual modulus values for specimens tested under isothermal fatigue conditions were 105 GPa (15.2 Msi) for those subjected to the triangular waveform compared to 112 GPa (16.2 Msi) for those subjected to the waveform including the hold time. For TMF tests, the average residual modulus values were 104 GPa (15.1 Msi) for material subjected to the triangular TMF profile and 112 GPa (16.2 Msi) for that subjected to the TMF profile including the hold time. There appeared to be no significant difference in the residual modulus among the four types of tests conducted in this investigation. However, these modulus values were, on the average, approximately 16% below modulus values obtained in room- and elevated-temperature tensile tests of the as-received composite material. Reasons for this reduction in modulus may rest on possible fiber debonding and loss of interfacial shear strength which occurred during fatigue testing. However, modulus does not appear to serve as a strong distinguishing characteristic among the final states of the material tested under the four fatigue conditions.

Figure 9 shows average residual strengths of the composite material. Under isothermal fatigue conditions, strengths were 343 MPa (49.7 ksi) for material subjected to the triangular isothermal profile and 308 MPa (44.7 ksi) for that subjected to the isothermal waveform with a hold time. Residual tensile tests on specimens subjected to TMF tests indicated average strengths were 364 MPa (52.8 ksi) for those subjected to the no-hold profile and 319 MPa (46.3 ksi) for those subjected to the profile

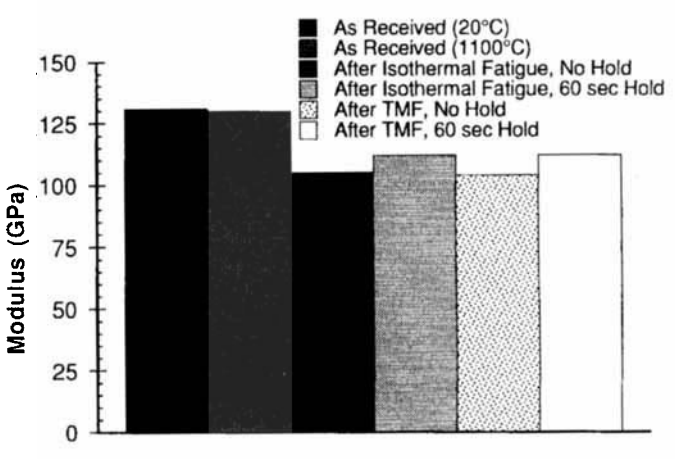

Fig. 8. Tensile modulus values for $[0]_{16}$ SiC/CAS-II subjected to various tensile, isothermal, and thermomechanical fatigue loading conditions.

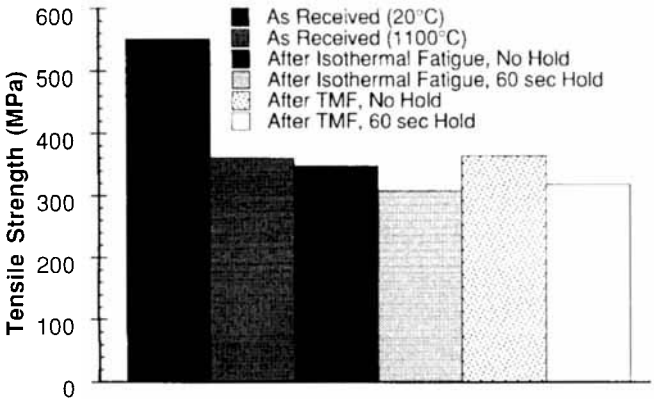

Fig. 9. Tensile strength values for $[0]_{16}$ SiC/CAS-II subjected to various tensile, isothermal, and thermomechanical fatigue loading conditions.

including the hold time. These average residual strength values range from 0% to 15% below the strength of the as-received SiC/CAS-II composite tested in tension at 1100°C and from 34% to 42% below its room-temperature tensile strength. The large difference in tensile strength between the room- and elevated-temperature tensile tests may be attributed, in part, to the difference in the residual stress states in the fiber and matrix at the beginning of each of these tests. For the room-temperature tensile test, the fibers are in compression, whereas for the elevated temperature tests they are in a near-zero stress state. If strain to failure in the fibers governs ultimate strength, and if fiber properties are not drastically affected by the test environment, the drop in strength at temperature is to be expected. Additionally, any decrease in matrix strength with temperature further contributes to the strength loss of the composite.

The only apparent trend in the residual strength data is the decrease in strength in the two tests conducted with the superimposed hold time. The accumulated strains, which are attributed to creep and which are significantly greater for the fatigue tests including the hold time, appear to be associated with this loss in strength but not with any change in modulus. The greater accumulated strains present in the material subjected to the tests including the hold time may result in a greater level of residual tension in the fibers following fatigue testing but prior to residual tensile testing. Following fatigue tests including hold times, the fibers are most likely in a state of residual tension. As discussed by Park and Holmes,[40] the tensile stress state of the fibers results from matrix creep slowly causing the fiber stress and strain to increase. Upon unloading following 1000 fatigue cycles, the matrix is placed into compression and the fibers into tension. This residual tensile stress state in the fibers appears to play a major role in reducing the residual tensile strength of this material. However, such a small difference in residual strength values implies that residual strength is not a sensitive indicator of accumulated fatigue damage for short-duration TMF loading such as that investigated for this project.

(6) States of Stress in Fiber and Matrix

Two methods were used to calculate the states of stress in the fiber and matrix: a one-dimensional uniaxial "rule of mixtures" approach, and an elastic, axisymmetric generalized plane-strain model, often referred to as a "concentric cylinder" model. Linear elastic material behavior was assumed in both approaches. Creep effects were not included. Because of this, their use was limited to determining the states of residual stress present in the composite constituents after processing and in estimating stress levels during the initial portions of testing. Whereas the uniaxial approach is able to predict only axial stresses in the fiber and matrix, the axisymmetric model can predict axial, radial, and circumferential stresses in the composite constituents. Both models account for applied mechanical stresses and thermally induced stresses.

Table III presents the stress states computed for the fiber and matrix under specific temperature and loading conditions. The CTE mismatch between the fiber and matrix results in a compressive residual stress in the fiber and a tensile residual axial stress in the matrix at room temperature. The axisymmetric model also shows that the fiber develops compressive stresses in the radial and circumferential directions, suggesting an increase in fiber–matrix interfacial strength with a decrease in temperature from the processing temperature. The increase in circumferential stress at room temperature supports the observation of smaller lengths of fiber pullout in room-temperature tensile tests.

Fiber and matrix stresses were also computed for the fatigue cycles used in this project using the axisymmetric model. Figures 10 and 11 show the computed axial stresses for the initial portions of the isothermal and thermomechanical profiles. Note that the axial stresses are in phase. Because of the increase in accumulated strain and postulated creep effects over the course of the tests, the predicted stress states portrayed in Figs. 9 and 10 are valid only during the initial portion of each test when linear elasticity may still be assumed. Later portions of each fatigue test appear to be affected by matrix creep causing the fiber stress to increase gradually while the matrix stress decreases proportionally.

In the isothermal tests (Fig. 10), the fibers sustained a maximum axial stress amplitude nearly twice as great as the matrix. Radial and circumferential stresses in the fiber and matrix were relatively lower (see Table III).

In contrast, the thermomechanical fatigue tests (Fig. 11) subjected the fiber to a nearly fully reversed stress profile, resulting in a stress amplitude over 750% greater than that sustained by the matrix. Table III shows that the circumferential and radial stresses were also greater than in the isothermal tests. Because the maximum temperature of the TMF cycle is the same as that in the isothermal tests, and the same maximum load is applied in both tests, the maximum fiber and matrix stresses are identical in both test types. The magnitude of the maximum axial stress in the fibers, though far greater than that in the matrix, is still relatively low compared to the threshold creep stress at 1100°C (600 MPa) reported by Simon and Bunsell[41] for ceramic-grade Nicalon.®

(7) Damage

Damage assessment is based on observations of the degradation of a specific mechanical property of a material throughout the course of a test. For ceramic matrix composites, such a property may be strength, strain, crack spacing, modulus, or another parameter. For fatigue testing, it is often beneficial to choose a property which can be analyzed during a test such as modulus or crack spacing rather than one which requires a post-fatigue evaluation such as residual strength or residual modulus. In this investigation, modulus, residual modulus, residual strength, and accumulated strain were evaluated as possible damage indicators for the tests conducted.

During the course of a TMF test, the temperature and modulus of a material change. This changing modulus makes it extremely difficult to numerically compare the moduli obtained from TMF hysteresis loops to those determined for the material from isothermal tensile tests. In this investigation, a hysteretic or "effective" modulus was taken as the slope of a straight line between the point of minimum stress, minimum strain, and the point of maximum stress, maximum strain on a hysteresis curve. Just as the modulus of a composite is used to monitor damage during conventional fatigue tests, the "effective" modulus was used in this study to observe the damage resulting from isothermal and thermomechanical fatigue testing.

Values of the "effective" modulus during isothermal and thermomechanical fatigue tests revealed no appreciable degradation during the course of the tests. The lack of an observed reduction in stiffness suggests that little or no fiber breakage occurred and that no matrix cracking was present. This supports the conclusion that the major contributor to the material

Table III. Fiber and Matrix Stress States*

Temp. (°C)	$\sigma_{applied}$ (MPa) [ksi]	Uniaxial model		Axisymmetric model					
		σ_{fz} (MPa) [ksi]	σ_{mz} (MPa) [ksi]	σ_{fz} (MPa) [ksi]	σ_{fr} (MPa) [ksi]	$\sigma_{f\theta}$ (MPa) [ksi]	σ_{mz} (MPa) [ksi]	$\sigma_{mr}^{\dagger}$ (MPa) [ksi]	$\sigma_{m\theta}^{\dagger}$ (MPa) [ksi]
20	0	−104.0 [−15.1]	69.6 [10.1]	−129.0 [−18.7]	−52.7 [−7.6]	−52.7 [−7.6]	86.1 [12.5]	−52.7 [−7.6]	123.0 [17.8]
500	0	−64.0 [−9.3]	42.7 [6.2]	−79.1 [−11.5]	−32.3 [−4.68]	−32.3 [−4.68]	52.8 [7.7]	−32.3 [−4.68]	75.4 [10.9]
500	10 [1.45]	−49.8 [−7.2]	49.9 [7.2]	−65.0 [−9.4]	−32.5 [−4.7]	−32.5 [−4.7]	60.0 [8.7]	−32.5 [−4.7]	75.7 [11.0]
1100	0	−11.9 [−1.7]	7.9 [11.5]	−14.7 [−2.1]	−6.1 [−0.9]	−6.1 [−0.9]	9.8 [1.4]	−6.1 [−0.9]	14.2 [2.1]
1100	10 [1.45]	2.0 [0.3]	15.3 [2.2]	−0.9 [−0.13]	−6.2 [−0.9]	−6.2 [−0.9]	17.3 [2.5]	−6.2 [−0.9]	14.6 [2.1]
1100	100 [14.5]	126.8 [18.4]	82.1 [11.9]	123.0 [17.8]	−7.6 [−1.1]	−7.6 [−1.1]	84.5 [12.2]	−7.6 [−1.1]	17.8 [2.6]

*Subscripts: f-fiber; m-matrix, z-axial, r-radial, θ-circumferential. †Measured at fiber–matrix interface.

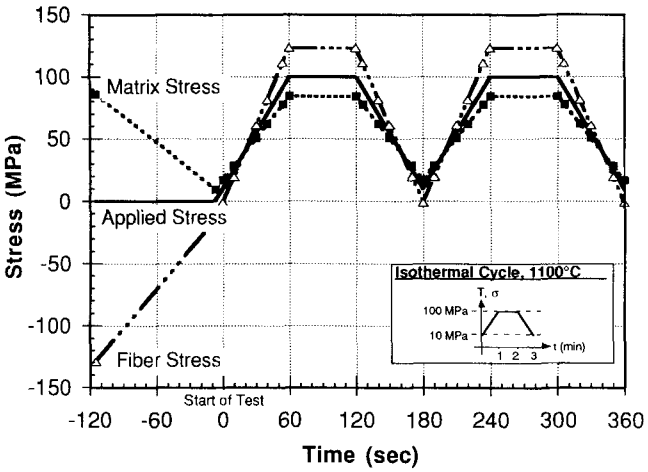

Fig. 10. Axial stress states in the fiber and matrix for an isothermal fatigue cycle including a 60-s hold at σ_{max} = 100 MPa, R = 0.1.

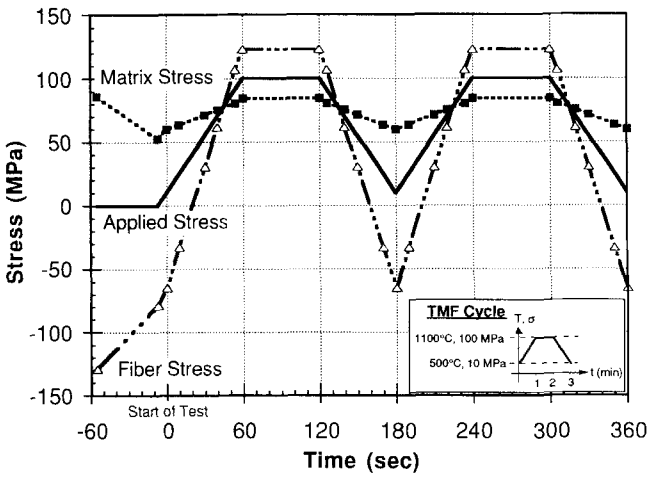

Fig. 11. Axial stress states in the fiber and matrix for a TMF cycle including a 60-s hold at σ_{max} = 100 MPa, R = 0.1, T = 500°–1100°C.

behavior was matrix creep. A stress analysis of the fiber supports this by indicating that the maximum axial fiber stress (approximately 123 MPa (17.8 ksi)) is far below the ultimate tensile strength of the fiber at 1100°C (approximately 1400 MPa (203 ksi)).[45]

Other parameters used for evaluating the state of damage of CMCs subjected to fatigue were the residual moduli (Fig. 8) and residual strengths (Fig. 9). As has been previously discussed, these postfatigue values did not show a clear distinguishing trend among the four types of fatigue investigated in this project. However, a change in a test parameter such as stress level, stress ratio, or temperature may result in damage that could more easily be identified using these residual property measurements.

Accumulated strain was the final quantity investigated as a damage indicator. Accumulated strains in the TMF tests were greater than for those in the isothermal fatigue tests under identical loading conditions. Furthermore, strain accumulated slightly more rapidly in the specimens subjected to the fatigue test with hold times. As discussed earlier, this quantity appears to be the most sensitive measure of damage accumulation during isothermal fatigue and TMF tests.

IV. Conclusions

This investigation has shown that the equipment and ability to conduct thermomechanical fatigue tests on ceramic matrix composites now exist. Though still requiring some modifications and improvements, test procedures and hardware are available to successfully evaluate the behavior of CMC systems under conditions simulating the aircraft gas turbine engine environment.

The most sensitive measure of changes in material behavior caused by the isothermal and thermomechanical fatigue profiles investigated was found to be strain accumulation. The addition of a hold time and cyclic temperature changes appeared to increase the initial strain accumulation rates and levels of strain accumulation observed in the material under the investigated fatigue parameters.

It is postulated that the primary cause of damage in this material under the specified conditions is matrix creep. Creep has been observed in this material at 1100°C,[43] and calculated average creep rates for the fatigue tests conducted are of the same order of magnitude. In addition, stress analyses of the fiber and matrix indicate that the fibers never reach a stress state above their creep threshold stress.

Results from the testing performed for this study and experience gained during its completion suggest several areas for further exploration. The use of noncontact strain and temperature measurement devices such as laser extensometers and optical pyrometers would be beneficial for future TMF tests. An effort should be made to optimize grip temperatures and thermal gradients in order to maximize the likelihood of obtaining gage section failures and of obtaining accurate strain-to-failure values. A larger data base of creep data for the fibers and matrix is

needed in order to more accurately model the thermomechanical behavior of this material. Finally, further testing should be performed to determine if the saturation level exhibited by the accumulated strain is truly indicative of a steady damage state at which components made from this material may be operated safely for long lives.

To compare the thermomechanical fatigue behavior of the SiC/CAS-II material with that of a metal–matrix composite, reference can be made to the work of Russ *et al.*[44] In-phase thermomechanical fatigue testing conducted on a unidirectional silicon carbide fiber-reinforced titanium aluminide composite (SCS-6/Ti–24Al–11Nb) showed its ability to endure 1000 or more cycles at higher stresses (500–900 MPa) but at much lower cyclic temperatures (150° to 650°C) than ceramic matrix composites can withstand. Clearly, the future use of such advanced materials as CMCs and MMCs depends upon careful selection of materials for their intended applications.

The thermomechanical fatigue regime is extremely important to materials research because of its significance in aerospace, power generation, and structural applications. Ceramic composites, as new materials proposed for use in hostile environments, must first be evaluated under extreme thermal and mechanical conditions prior to being approved for service. Though far from all-inclusive, this project has investigated the response of one type of ceramic matrix composite to a discrete set of thermomechanical fatigue parameters in an attempt to bring laboratory research closer to simulating the proposed operating environment for ceramic matrix composites.

References

[1]D. B. Marshall and A. G. Evans, "Failure Mechanisms in Ceramic Fiber/Ceramic Matrix Composites," *J. Am. Ceram. Soc.*, **68** [5] 225–31 (1985).

[2]O. Sbaizero and A. G. Evans, "Tensile and Shear Properties of Laminated Ceramic Matrix Composites," *J. Am. Ceram. Soc.*, **68** [6] 481–86 (1986).

[3]A. G. Evans and B. J. Dagleish, "Some Aspects of the High Temperature Performance of Ceramics and Ceramic Composites"; in *Advanced Materials for Severe Applications*. Edited by K. Iida and A. J. McEvily. Elsevier Applied Science Publishers, London, England, 1986.

[4]D. B. Marshall and B. N. Cox, "Tensile Behavior of Brittle Matrix Composites: Influence of Fiber Strength," *Acta Metall.*, **35** [11] 2607–619 (1987).

[5]M. D. Thouless and A. G. Evans, "Effects of Pull-Out on the Mechanical Properties of Ceramic Matrix Composites," *Acta Metall.*, **36** [3] 517–22 (1988).

[6]A. G. Evans and D. B. Marshall, "The Mechanical Behavior of Ceramic Matrix Composites," *Acta Metall.*, **37** [10] 2567–83 (1989).

[7]K. M. Prewo, "Fatigue and Stress Rupture of Silicon Carbide Fibre-Reinforced Glass-Ceramics," *J. Mater. Sci.*, **22,** 2695–701 (1987).

[8]K. M. Prewo, B. Johnson, and S. Starrett, "Silicon Carbide Fiber-Reinforced Glass Ceramic Composite Tensile Behavior at Elevated Temperature," *J. Mater. Sci.*, **24,** 1373–79 (1989).

[9]J. W. Holmes, T. Kotil, and W. T. Foulds, "High Temperature Fatigue of SiC Fiber Reinforced Si_3N_4 Ceramic Composites"; pp. 176–86 in *Symposium on High Temperature Composites*. American Society for Composites, Technomic Publishing Co., Lancaster, PA, 1989.

[10]C. Q. Rousseau, "Monotonic and Cyclic Behavior of a Silicon Carbide/Calcium Aluminosilicate Ceramic Composite"; pp. 136–51 in "Thermal and Mechanical Behavior of Metal Matrix and Ceramic Matrix Composites," ASTM STP 1080. Edited by J. M. Kennedy, H. H. Moeller, and W. S. Johnson. American Society for Testing and Materials, Philadelphia, PA, 1990.

[11]J. W. Holmes, "Influence of Stress Ratio on the Elevated-Temperature Fatigue of a Silicon Carbide Fiber-Reinforced Silicon Nitride Composite," *J. Am. Ceram. Soc.*, **74** [7] 1639–45 (1991).

[12]L. P. Zawada, L. M. Butkus, and G. A. Hartman, "Room Temperature Tensile and Fatigue Properties of Silicon Carbide Fiber-Reinforced Aluminosilicate Glass," *J. Am. Ceram. Soc.*, **74** [11] 2851–58 (1991).

[13]L. P. Zawada and R. C. Wetherhold, "The Effects of Thermal Fatigue on a SiC Fibre/Aluminosilicate Glass Composite," *J. Mater. Sci.*, **26,** 648–54 (1991).

[14]F. Abbe, J. Vincens, and J. L. Charmant, "Creep Behavior and Microstructural Characterization of a Ceramic Matrix Composite," *J. Mater. Sci. Lett.*, **8** [9] 1026–28 (1989).

[15]J. W. Holmes, "Tensile Creep Behavior of a Fiber-Reinforced SiC-Si_3N_4 Composite," *J. Mater. Sci.*, **26** [11] 1808–14 (1991).

[16]C. Q. Rousseau, see Ref. 10, p. 137.

[17]Personal communication with R. Stewart, Corning, Inc., 1 October 1991.

[18]D. C. Larsen, S. L. Stuchly, and J. W. Adams, "Evaluation of Ceramics and Ceramic Composites for Turbine Engine Applications," AFWAL Technical Report AFWAL-TR-88-4202. Materials Laboratory, Air Force Wright Aeronautical Laboratories, Wright-Patterson AFB, OH, December 1988.

[19]R. A. Allaire, V. F. Janas, S. Stuchly, and M. P. Taylor, "Glass Matrix Composites for Higher Use Temperature Applications," *SAMPE Quarterly*, **19** [1] 29 (1987).

[20]R. A. Allaire, V. F. Janas, S. Stuchly, and M. P. Taylor; see Ref. 19, p. 25.

[21]A. Ma, J. W. Holmes, and M. Kidder, "Stress Analysis of an Edge-Loaded Ceramic Tensile Specimen," to be submitted to *J. Am. Ceram. Soc.*

[22]J. W. Holmes, "A Technique for Tensile Fatigue and Creep Testing of Fiber-Reinforced Ceramics," *J. Comp. Mater.*, **26** [6] 915–32 (1992).

[23]J. W. Holmes, "Influence of Stress Ratio on the Elevated-Temperature Fatigue of a Silicon Carbide Fiber-Reinforced Silcon Nitride Composite," *J. Am. Ceram. Soc.*, **74** [7] 1641 (1991).

[24]R. W. Goettler and K. T. Faber, "Interfacial Shear Stresses in SiC and Al_2O_3 Fiber-Reinforced Glasses," *Ceram. Eng. Sci. Proc.*, **9** [7–8] 864 (1988).

[25]J. W. Holmes, F. A. McClintock, K. S. O'Hara, and M. E. Conners, "Thermal Fatigue Testing of Coated Monocrystalline Superalloys"; p. 672 in "Low Cycle Fatigue," ASTM STP 942. Edited by H. D. Solomon, G. R. Halford, L. R. Kaisand, and B. N. Keis. American Society for Testing and Materials, Philadelphia, PA, 1985.

[26]G. A. Hartman, L. P. Zawada, and S. M. Russ, "Techniques for Elevated Temperature Testing of Advanced Ceramic Composite Materials"; pp. 31–38 in *Fifth Annual Hostile Environments and High Temperature Measurements Conference Proceedings*. Society for Experimental Mechanics, Englewood Cliffs, NJ, 1988.

[27]G. A. Hartman and S. M. Russ, "Techniques for Mechanical and Thermal Testing of Ti3Al/SCS-6 Metal Matrix Composites"; pp. 43–53 in "Metal Matrix Composites: Testing Analysis, and Failure Modes," ASTM STP 1032. Edited by W. S. Johnson. American Society for Testing and Materials, Philadelphia, PA, 1989.

[28]L. M. Butkus, L. P. Zawada, and G. A. Hartman, "Fatigue Test Methodology and Results for Ceramic Matrix Composites at Room and Elevated Temperatures"; pp. 52–68 in "Cyclic Deformation Fracture, and Nondestructive Evaluation of Advanced Materials," ASTM STP 1157. Edited by M. R. Mitchel and O. Buck. American Society for Testing and Materials, Philadelphia, PA, 1992.

[29]G. A. Hartman and N. E. Ashbaugh, "A Fracture Mechanics Test Automation System for a Basic Research Laboratory"; pp. 95–110 in "Applications of Automation Technology to Fatigue and Fracture Testing," ASTM STP 1092. Edited by A. A. Braun, N. E. Ashbaugh, and F. M. Smith. American Society for Testing and Materials, Philadelphia, PA, 1990.

[30]L. P. Zawada, L. M. Butkus, and G. A. Hartman, "Room Temperature Tensile and Fatigue Properties of Silicon Carbide Fiber-Reinforced Aluminosilicate Glass," *J. Am. Ceram. Soc.*, **74** [11] 2851–58 (1991).

[31]S.-W. Wang and A. Parvizi-Majidi, "Mechanical Behavior of Nicalon Fiber Reinforced Calcium Aluminosilicate Matrix Composites," *Ceram. Eng. Sci. Proc.*, **11** [9–10] 1608 (1989).

[32]T. R. Barnett and H. S. Starrett, "Room and Elevated Temperature Mechanical and Thermal Properties of Corning Nicalon/CAS," WRDC Technical Report WRDC-TR-90-4131; pp. 73–74. Materials Directorate, Wright Laboratory, Wright-Patterson AFB, OH, February 1992.

[33]J. W. Holmes, "Experimental Observations of Frictional Heating in Fiber-Reinforced Composites," *J. Am. Ceram. Soc.*, **75** [4] 929–38 (1992).

[34]D. S. Beyerle, S. M. Spearing, F. W. Zok, and A. G. Evans, "Damage and Failure in Unidirectional Ceramic-Matrix Composites," *J. Am. Ceram. Soc.*, **75** [10] 2719–25 (1992).

[35]M. D. Thouless, O. Sbaizero, L. S. Sigl, and A. G. Evans, "Effect of Interface Mechanical Properties on Pullout in a SiC-Fiber-Reinforced Lithium Aluminum Silicate Glass-Ceramic," *J. Am. Ceram. Soc.*, **72** [4] 525–32 (1989).

[36]E. Bischoff, M. Rühle, O. Sbaizero, and A. G. Evans, "Microstructural Studies of the Interfacial Zone of a SiC Fiber-Reinforced Lithium Aluminum Silicate Glass-Ceramic," *J. Am. Ceram. Soc.*, **72** [5] 741–45 (1989).

[37]"CoaxCyl5E," developed by Dr. T. Hahn, Naval Research Laboratory, Washington, DC. Modified by D. Coker, The University of Dayton Research Laboratory, Dayton, OH.

[38]U. V. Deshmukh, A. Kanei, S. W. Freiman, and D. C. Cranmer, "Effect of Thermal Expansion Mismatch on Fiber Pull-out in Glass Matrix Composites"; pp. 253–58 in *High Temperature/High Performance Composites*, Materials Research Society Symposium Proceedings, Vol. 120. Edited by F. D. Lemkey, S. G. Fishman, A. G. Evans, and J. R. Strife. Materials Research Society, Pittsburgh, PA, 1988.

[39]L. M. Butkus, L. P. Zawada, and G. A. Hartman, "Room Temperature Tensile and Fatigue Behavior of Silicon Carbide Fiber-Reinforced Ceramic Matrix Composites"; presented at AeroMat '90. ASM International, Long Beach, CA, May 1990.

[40]Y. Park and J. W. Holmes, "A Finite Element Model of Creep Deformation in Fiber-Reinforced Ceramic Composites," *J. Mater. Sci.*, in press.

[41]G. Simon and A. R. Bunsell, "Mechanical and Structural Characterization of the Nicalon Silicon Carbide Fibre," *J. Mater. Sci.*, **19** [11] 3649–57 (1984).

[42]M. A. Rigdon and W. S. Hong, "Comparison of High-Temperature Testing Results of Ceramic Fibers"; pp. 136–51 in "Thermal and Mechanical Behavior of Metal Matrix and Ceramic Matrix Composites," ASTM STP 1080. Edited by J. M. Kennedy, H. H. Moeller, and W. S. Johnson. American Society for Testing and Materials, Philadelphia, PA, 1990.

[43]J. W. Holmes and J. W. Jones, University of Michigan; unpublished data.

[44]S. M. Russ, T. Nicholas, M. Bates, and S. Mall, "Thermomechanical Fatigue of a SCS-6/Ti-24Al-11Nb Metal Matrix Composite"; to be published in *Failure Mechanisms in High Temperature Composites*, Proceedings of the American Society of Mechanical Engineers Symposium, Atlanta, GA, December, 1991. American Society of Mechanical Engineers, New York, NY, 1992. □